

Revision of the paper HESS-2017-196

We would like to thank to both the anonymous reviewers for the thoughtful comments provided to our manuscript. A point-to-point reply to major and minor comments is reported below, as well as indication of the changes made to the text to address such comments.

Reply to Referee #1 Comments

General

This study investigates the potential of one model-based and two remotely sensed datasets for their use in an established global drought monitoring system. The study uses soil moisture from the Lisflood model, surface soil moisture from the microwave-based ESA CCI soil moisture dataset and land Surface temperature from MODIS. Random errors of these datasets are characterized with the triple collocation analysis (TCA), a firmly established method in soil moisture analysis. As such, apart from applying the TCA to a different triple of datasets, the study is not very innovative. However, since the datasets are expected to be used in an operational drought monitoring system, the results of this study are expected to have a large practical impact. This study is performed in a scientifically sound and clearly structured way and provide some interesting insights in the skill of the datasets considered. I therefore recommend its publication after addressing the following issues.

Thanks for your comment. Regarding the innovative aspect of the work, we agree that the application of triple collocation is nothing new in the scientific literature of soil moisture; however, there are very few studies analyzing modelled, microwave and thermal data, and none of them are focusing on the study areas reported here. Additionally, the use of standardized anomalies in TCA is uncommon in the literature even if it is a key aspect in drought studies. As you stated, the final goal of the study is to provide insight on the spatial distribution of the errors in our global drought observatory, hence the analysis of these three specific datasets (previously uninvestigated in TCA literature) and anomaly values is a novelty and a key requirement of our study. We clarified these novelties of the study in the new introduction section of the paper.

Major comments

1. The analyses in this study are based on monthly anomalies. Although theoretically it is feasible to do so, I wonder what the practical relevance of these results are. All datasets used are also available at a daily time step and already now the European Drought Observatory works with ten-day periods (dekades). Hence, also the error structures should be known at these time scales.

The use of time-aggregated data is a common practice in drought analyses in order to ensure the statistical robustness of the computed anomalies. Daily values are often too noisy to allow for a robust statistical analysis. The use of a monthly temporal scale is quite common in the drought literature, and it has been preferred (at the moment) over the ten-day scale (adopted in EDO) for operational/technical reasons. Indeed, the monthly time scale will be the one implemented in the GDO system as a first approach. Higher temporal resolutions will be tested and implemented in the future. We clarified this point in the revised version of the manuscript.

2. I was expecting a more thorough analysis on the consequences of using three datasets that represent very different layer depths, i.e.:

* ESA CCI soil moisture represents the upper 2 cm, * LST represents the skin temperature, which is driven both by surface soil moisture (influencing bare soil temperature) and root zone soil moisture (impacting vegetation canopy temperature) * LIS represents root zone soil moisture (but layer depth is not provided in the manuscript).

Typically, deeper and thicker layers have lower random errors than observations of the surface layer, but this also depends on the time scale you're looking at (e.g. daily observations typically have larger random errors than monthly averages). Is there a way you can test the impact of using such different layer depths, e.g. by using the surface layer of LISFLOOD?

We agree that the different vertical (as well as horizontal) resolution of the three datasets may lead to some discrepancies in the analysis. For this reason, we elaborated the data in order to try to minimize the possible discrepancies among the datasets. For instance, the use of monthly aggregated data is one of the techniques adopted to ensure minimizing the discrepancies between the three datasets related to the slower response of deeper soil layers (as you highlighted). Also, the use of standardized quantities allows reducing the effects of possible biases between soil moisture modelled at different depths.

We modified the text to highlight further the expedients adopted to try to minimize those issues, as well as highlighting where the different resolutions may lead to a better performance of one dataset over the others.

3. Some important information is missing (or not clearly provided) which is needed for a correct interpretation of the results: in which units are the TCA results expressed? Is it the fractional RMSE? If not, are the errors of each dataset expressed in its own data space or in a common data space provided by one of the models?

We better clarified that the errors are provided as dimensionless quantities (multiple of standard deviation), due to the standardization applied to the three datasets before performing the TCA. The standardization procedure also allows having all the three datasets in the same range of variability

(zero mean, unitary standard deviation), which removes the need of a reference data space. Additionally, as briefly stated in the “Methods” section, we adopted the TCA “covariance notation”, which does not require a common (arbitrary) reference dataset. We highlighted that information in the revised text.

Minor Comments

Line 16: why do you use the word proxy here? Only LST can be considered a proxy of soil moisture, while both LIS and ESA CCI are real estimates of soil moisture.

We rephrased this sentence.

Line 20: The official name is ESA CCI Soil Moisture or ESA CCI SM.

We reworded this definition of the product.

line 43: When agricultural droughts start affecting human welfare, people commonly use the term socioeconomic drought.

In our opinion, socioeconomic drought is a much larger concept that includes also other economic factors and that is separated from the classical “physical” classification meteorological/hydrological/agricultural. We prefer to leave this sentence as it is.

Lines 47/48: include references or URLs to these drought monitoring systems.

Done.

Lines 51/52: these citations refer to the formulation of drought indices rather than soil moisture.

We clarified that we were referring to soil moisture modelling in the context of drought.

Lines 83-97: please provide references to the various datasets discussed here (MODIS LST, ESA CCI SM, LISFLOOD).

References are reported in the successive sub-sections dedicated to each product. We prefer to leave this part of the introduction easy to read by avoiding further references.

Regarding the skill of LST-based soil moisture versus ESA CCI SM the authors should also refer to the ALEXI-based work of Fang et al. 2016 (<http://www.sciencedirect.com/science/article/pii/S0303243415300404>).

Thanks. We added some comments on this work in the results section.

Line 93: ESA CCI SM will soon be updated in NRT in the framework of Copernicus Climate Change Services (<http://www.sciencedirect.com/science/article/pii/S0303243415300404>).

Yes, we added this information to the text.

Line 97: The use of the term "models" is confusing and only applies to Lisflood. Replace "models" with "datasets" or "products", also throughout the rest of the manuscript.

Done.

Line 120: No definition is given of the root zone soil moisture simulated with Lisflood. What soil column is sampled?

Information have been added to sub-section 3.1.

line 128: I don't see how Pearson R would give information about the slope and biases between two datasets. Do you confuse it with the "regression function" between the datasets?

This is true only for the specific case of a regression analyses between two standardized quantities with zero mean and a unitary variance. The text has been amended to clarify this point.

Line 130: to my knowledge the correct name for this test is Student's t-test.

Done.

Line 148: spelling error: where -> were.

Done.

Line 168: it is unclear why you don't use the surface layer, which is much closer to the other two data sets. I suggest to repeat the TCA with the surface layer as well to see what impact is on the estimated errors of all datasets.

We agree that the LIS surface layer is closer to CCI but not necessarily to LST (which depth depends on vegetation coverage). We preferred root zone because it is more relevant for agricultural drought studies. Currently, we are testing the value of extrapolated "root-zone-like" soil moisture from skin CCI values, but this analysis is going beyond the goal of this paper.

Line 204: It may be worth checking whether using Microwave-based LSTs would lead to similar results (See Holmes et al., 2009; <http://onlinelibrary.wiley.com/doi/10.1029/2008JD010257>).

We are aware of the studies on microwave LST, but we do not think that these are relevant in this specific case study, since they compare quite well with MODIS data under clear sky conditions. The main advance of microwave-based LST dataset is to remove the limitation of thermal data during cloudy days, which is not impactful at monthly time scale. Also, microwave data have, at the moment, a coarser spatial resolution.

Line 225: provide version number of "current" version.

Done.

Line 233: Please check Terms and Conditions (<http://www.esa-soilmoisture-cci.org/dataregistration/terms-and-conditions>) for a correct citation of the data.

References have been updated.

Line 236-237: Only for the integration of SSM/I into the merged products the soil moisture signal is decomposed into seasonality and anomalies (Liu et al. (2012)).

Yes, you are right. However, this is just a very brief summary of the procedure and we think that the readers can find a very clear and detailed description of the procedure (if they are interested) in the cited paper.

Line 253: it is not clear whether the linear correlation is computed from the original signal or from the anomalies. Since your TCA implementation is based on the anomalies, also the correlation computation should be based on these.

Yes, it is computed on the anomalies. We clarified this in the text.

Line 282-283: Is the stronger correlation between CCI and LST not expected, as they represent more closely related soil layers? This is something you could test by including also the surface layer of Lisflood in your analysis.

In the new version of the text we added more considerations related to the explored vertical depth of each dataset. Yes, indeed it is expected that LST performs more closely to CCI in low-coverage areas (like Australia) and more closely to LIS over more vegetated areas.

Line 307: On one hand -> On the one hand.

Done.

Line 331: the results of this manuscript cannot be directly compared to those of Pierdicca et al., since the latter applies the TCA to daily observations.

Yes, this is true. This is the reason why we highlighted only some qualitative analogies. We clarified this difference in the two studies in the new version of the text.

Line 397: For what is skin soil moisture more reliable? Do you mean the estimates themselves? The estimation of soil moisture from microwave remote sensing may have large uncertainties over dry areas (e.g. Hahn et al., 2017: <http://ieeexplore.ieee.org/document/7815274/>).

We agree that under some circumstances microwave products can have large uncertainties over dry sandy soil. We rephrased the sentence to clarify that the presence of vegetation generally tends to reduce the reliability of microwave estimates.

Line 406: There are several studies that combine various datasets with different error characteristics, e.g. Liu et al., 2011 (<http://www.hydrol-earth-syst-sci.net/15/425/2011/hess-15-425-2011.html>); Beck et al., 2017 (<http://www.hydrol-earth-syst-sci.net/21/589/2017/hess-21-589-2017.html>); Yilmaz et al; 2012 (<http://onlinelibrary.wiley.com/doi/10.1029/2011WR011682/full>). Is there something that you can learn from these studies for your application?

We cited most of the reported authors (even if not specifically these papers) in our text already. The majority of these (and other) merging procedures are loosely based on a weighted average approach, with weights derived from the error analysis procedure. Particularly, the approach proposed in Yilmaz et al. (2012) is the one that we are currently implementing in our operational

system, of which this study is the error characterization step. We highlighted this in the final section of the new version of the manuscript and we added some maps showing the actual spatial distribution and frequency of the weighting factors, as also suggested by rev. #2.

Reply to Referee #2 Comments

In the paper titled “Comparing soil moisture anomalies from multiple independent sources over different regions across the globe” authors have investigated the anomaly components of three products and then compared the errors of the standardized products over five different regions. Overall, the manuscript is written well and appropriate to the journal Hydrology and Earth System Sciences. However, there are some parts still need improvement:

- There are other soil moisture inter-comparison studies performed before at global scale, including the ones that have already implemented TCA. First of all authors should explicitly justify the need of anomaly comparisons at large scales (i.e., not performed before over these locations using anomalies?). It is not all that clear what additional benefit do readers get from this study compared to the earlier studies (i.e., the analysis performed here are not performed before?). What is the new thing? Datasets? Locations? Anomaly components investigated instead of entire datasets? The information given in the introductions should better be tied with the overall goal.

We modified most of the final part of the introduction in order to highlight the novelty and the motivation of this study, as also requested by Rev. #1. In summary, most of the past TC studies were focused on soil moisture data rather than anomalies, with the latter being a key variable for drought monitoring that can behave quite differently from soil moisture itself. The inclusion of thermal remote sensing datasets is quite rare in the TC literature, and no studies on global scale are available to our knowledge. It follows that, even if the methodology adopted can be considered “standard”, the data analyzed here are unique in terms of both variable investigated and datasets adopted. Finally, the operational focus of this study (error analysis to be used in a future implementation in a near-real time monitoring system) requires analyzing specifically those datasets that can be actually used in the GDO monitoring system.

What is the vertical support of the soil moisture product comparison performed here considering modeled soil moisture reflect root-zone while the MODIS LST and ESA CCI soil moisture products reflect the top couple cm depths. How does it relate to the overall framework of the study (agricultural drought monitoring while root-zone soil moisture lies at the hearth of such analyses in general)? Surface skin soil moisture is a good indicator for agricultural drought?

As replied to the second major comment of rev. #1, we adopted some pre-processing procedures in order to minimize likely discrepancies between datasets with different vertical resolution. In this context, the choice of a monthly-aggregation period aimed at removing the time shift between data referring to different soil depths, whereas standardized anomalies removed biases among the three datasets. The obtained results seem to support the idea that these expedites were able to make the datasets comparable overall.

These considerations were further highlighted in the new version of the manuscript.

Percentage error variance information is not all that helpful, perhaps actual standard deviations (volumetric error for the model and satellite soil moisture products and K for the LST product) would be more helpful (i.e., how do these errors relate to specific mission goals of 4%). Or at least authors should justify why presentation of standardized error variance is a better thing to do compared to actual error variance.

Actual error variance (i.e., in terms of volumetric water content or degree) cannot be reported in this study, since standardized variables (normalized z-scores) are investigated for the above mentioned reasons. The use of standardized quantities is justified by the needs of drought monitoring, as clarified in the new version of the manuscript.

Error variance comparisons of three datasets in space is done, but it would be helpful if more is given. For example, specific pattern between the error variance and vegetation/precipitation/elevation distributions? Any one better under such and such conditions (instead of only locations)? Why better? A dedicated paragraph would be very helpful.

We agree that it would be helpful to be able to provide more insight on the spatial patterns of the errors. However, the obtained results do not provide clear evidence of the suggested relations, behind some general behaviors (LIS perform better over well-monitored agricultural areas whereas CCI perform better over remote dry areas). We highlighted the inability to infer further on spatial patterns on the new version of the discussion and conclusion sections.

Combination of different datasets is spelled out in the introduction (final paragraph where the goal of the study is stated) but not performed (it gives the impression that this study will merge different products; perhaps it should have given all the necessary inputs are available including the error sources of each product).

We agree that this sentence may be misleading, and we rephrased the text to clarify this point. Even if the final goal of our project is to provide an operational ensemble product for drought monitoring, the goal of this specific study is "limited" to the characterization of spatial errors for the three selected datasets. The output of this error analysis is used to obtain statistical robust weighting factors for a reliable ensemble product to be used in GDO, and maps of these weighting factors have

been added to the new version of the manuscript. Indeed, a first version of this product is already available in a prototype form in GDO, but a full implementation of the ensemble (based on the outcome of this study) is subordinate to the future availability of CCI in near-real time.

In the new version of the manuscript we clarified that the ensemble product is not the final goal of the reported study, but that the goal of the research is to spatially characterize the errors to be used in the future within the operational system. However, more details on the weighting factor have been added to partially fulfil your request.

Some background discussion about the TCA dataset requirements/assumptions (e.g., length? See Zwieback et al, 2012, doi:10.5194/npg-19-69-2012).

We added these considerations to the methods section, as well as some relevant references.

L98: “two folds” L102: “to develop a suitable combination procedure for a near-real time detection of the occurrence of ecosystem drought events”.. More specifics. How this will be performed? Using TCA errors to calculate the weights in a merging algorithm?

Yes. As now clarified in the text, the merging procedure will be based on a weighted average with weights derived from the TC errors. Details on the spatial distribution of the weighting factors have been added; however, the implementation of such ensemble product is not yet fully developed in the operational GDO system.

L112: revise “in order to make directly comparable the different datasets”.

Done.

1 Comparing soil moisture anomalies from multiple independent sources over 2 different regions across the globe

3
4 Carmelo Cammalleri, Jürgen V. Vogt, Bernard Bisselink, Ad de Roo

5 European Commission, Joint Research Centre (JRC), Ispra, Italy.

6
7 *Correspondence to:* C. Cammalleri, European Commission - Joint Research Centre, via E. Fermi 2749,
8 I-21027 Ispra (VA), Italy. Bldg. ~~10026b~~, Room ~~1208140~~, TP ~~122267~~. Phone: +39 (0)332.78.9869, e-
9 mail: carmelo.cammalleri@ec.europa.eu.

10
11 **Abstract:** Agricultural drought events can affect large regions across the World, implying the urge for a
12 suitable global tool for an accurate monitoring of this phenomenon. Soil moisture anomalies are
13 considered a good metric to capture the occurrence of agricultural drought events, and they have
14 become an important component of several operational drought monitoring systems. In the framework
15 of the JRC Global Drought Observatory (GDO, <http://edo.jrc.ec.europa.eu/gdo/>) the suitability of
16 ~~modelled and/or satellite derived proxy of soil moisture anomalies of a~~ was investigated. ~~In this study,~~
17 three datasets ~~have been evaluated~~ as possible ~~proxies representation~~ of root zone soil moisture
18 anomalies has been evaluated: (1) soil moisture from the Lisflood distributed hydrological model
19 (namely LIS), (2) remotely sensed ~~land-Land surface-Surface temperature-Temperature~~ data from the
20 MODIS satellite (namely LST), and (3) the ESA Climate Change Initiative combined passive/active
21 microwave skin soil moisture dataset ~~_developed by ESA_~~ (namely CCI). Due to the independency of
22 these three datasets, the Triple Collocation (TC) technique has been applied, aiming at quantifying the
23 likely error associated to each dataset in comparison to the unknown true status of the system. TC
24 analysis was performed on five macro-regions (namely North America, Europe, India, Southern Africa
25 and Australia) detected as suitable for the experiment, providing insight into the mutual relationship
26 between these datasets as well as an assessment of the accuracy of each method. Even if no definitive
27 statement on the spatial distribution of errors can be provided, Aa clear outcome of the TC analysis is

28 the good performance of remote sensing datasets, especially CCI, over dry regions such as Australia and
29 Southern Africa, whereas the outputs of LIS seem to be more reliable over areas that are well monitored
30 through meteorological ground station networks, such as North America and Europe. In a global
31 drought monitoring system, these results ~~of the error analysis can be~~ used to design a weighted-
32 average ensemble system that exploits the advantages of each dataset.

33

34 1. Introduction

35

36 Drought is a recurring natural extreme, triggered by lower than normal rainfall, often exacerbated
37 by a strong evaporative demand due to high temperatures and strong winds. Drought events may occur
38 in all climates and in most parts of the world, since drought is defined as a temporary deviation from the
39 local normal condition. Due to the usually wide extension of the interested area, drought affects millions
40 of people across the Globe each year (Wilhite, 2000).

41 On the basis of the economic and natural sectors impacted by this phenomenon, a drought event is
42 usually classified in meteorological, agricultural and hydrological drought, depending on the persistence
43 of the water deficit within the hydrological cycle. Of particular interest for this study are the agricultural
44 (or ecosystem) drought events, defined as prolonged periods with drier than usual soils that negatively
45 affect vegetation growth and crop production, and, as a consequence, human welfare (Dai, 2011).

46 Soil moisture is commonly seen as one of the most suitable variables to monitor and quantify the
47 impact of water shortage on vegetated lands due to its effects on the terrestrial biosphere and the
48 feedback into the atmospheric system, as highlighted by the inclusion of time-aggregated soil moisture
49 anomalies (e.g., monthly) in numerous drought monitoring systems at regional to continental scales
50 (i.e., European Drought Observatory, <http://edo.jrc.ec.europa.eu>; United States Drought Monitor,
51 <http://droughtmonitor.unl.edu>; African Flood and Drought Monitor,
52 <http://hydrology.princeton.edu/adm/>; among others).

53 In the context of drought monitoring, the Ssoil moisture ~~monitoring dynamic~~ over large areas is
54 usually ~~obtained modelled~~ through either distributed hydrological models or land-surface schemes of

55 climate models (Crow et al., 2012; Sheffield et al., 2004), as well as by thermal or passive/active
56 microwave remote sensing-derived quantities (see e.g., Anderson et al., 2007; Houborg et al., 2012; Mo
57 et al., 2010). ~~Particularly, with regards to a the context of a global-scale drought monitoring~~
58 ~~system monitoring~~, remote sensing-based approaches have the advantage of an intrinsic worldwide
59 coverage, but the drawbacks, in the case of microwave sensors, of exploring only the first few
60 centimeters of soil and a decreasing sensitivity with the increase of vegetation coverage (Jackson,
61 2006). In the case of thermal data, the lack of coverage during cloudy conditions and the nontrivial
62 connection between thermal and soil moisture signals (Price, 1980) are other limitations. On the
63 contrary, diagnostic models allow for a continuous monitoring of soil moisture at the desired soil
64 depths, but the accuracy of the data is constrained by uncertainties in the parameterization of soil
65 hydrological characteristics, as well as by the actual availability of near-real time reliable
66 meteorological forcing data. Generally, the use of in-situ observations for large area monitoring is
67 limited, mainly due to the lack of long records, the sparseness of recording stations and the high spatial
68 heterogeneity of soil moisture fields.

69 It follows that both satellite measurements and model predictions are subject to errors and
70 uncertainties that need to be accounted for in their interpretation and application (Gruber et al., 2016).
71 This also suggests that a monitoring system based on a single model is rarely capable to provide global
72 reliable estimates, and a combination of different data sources is desirable in order to minimize the
73 errors in the detection of drought events. Recently, Cammalleri et al. (2015) demonstrated the value of
74 an ensemble of modelled soil moisture anomalies for drought monitoring over Europe, similarly to the
75 findings of the U.S. National Land Data Assimilation System (NLDAS) (Dirmeyer et al., 2006).
76 However, a key point in combining different modelled data is the need to estimate the affinity and
77 divergence between the models across the modelling domain.

78 In the most recent years, the Triple Collocation (TC) technique (Stoffelen, 1998) has been
79 established as a practical approach to evaluate the unknown error variance (with respect to the truth) of
80 three mutually independent measurement systems without knowing the “true” status of the system
81 (Yilmaz and Crow, 2014). This technique has been widely applied in hydrology to estimate errors in

82 soil moisture, as well as to evaluate precipitation and vegetation property indicators (Dorigo et al.,
83 2010; McColl et al., 2014). One key requirement in TC is the existence of linearity between the three
84 estimates and the truth, which can fail in the case of strongly seasonal geophysical variables such as soil
85 moisture (Su et al., 2014). Luckily, drought monitoring systems are usually based on soil moisture
86 anomalies rather than actual values, hence providing a partial remedy to this problem and making soil
87 moisture anomalies directly suitable for this methodology (Miralles et al., 2010). However, since most
88 of TC studies focused on soil moisture dynamics rather than standardized anomalies, specific analyses
89 are required to evaluate ~~spatially~~ the accuracy of each dataset across the spatial domain.

90 In the frame of an operational monitoring of agriculture and ecosystem drought, the availability of
91 soil moisture, or proxy, datasets available in near-real time is crucial; within the Global Drought
92 Observatory (GDO, <http://edo.jrc.ec.europa.eu/gdo/>), developed by the Joint Research Centre (JRC) of
93 the European Commission, the soil moisture outputs of the Lisflood hydrological model and the land
94 surface temperature (LST) anomalies derived from the Moderate-Resolution Imaging Spectroradiometer
95 (MODIS) onboard the Terra satellite have been detected as suitable datasets for a near-real time
96 monitoring. In particular, Cammalleri and Vogt (2016) have highlighted how monthly-average LST
97 anomalies represent the best proxy of soil moisture variations across different climates in Europe when
98 compared to other LST-derived quantities.

99 As a third dataset for the TC analysis, the combined active/passive microwave soil moisture
100 dataset produced by the European Space Agency (ESA) in the context of the Climate Change Initiative
101 (CCI) is used; even if this dataset is not currently updated in near-real time, it represents a valuable
102 reference dataset for a global consistent time-series of microwave-based soil moisture maps (also, near-
103 real time updating is foreseen in the framework of the Copernicus Climate Change Services).

104 The agreement between ~~of~~ anomaly time-series derived from these three products ~~has~~ not been
105 fully investigated in the literature, especially at global scale; hence, given the independency of the three
106 sources of data ~~The use of three independent sources of data~~ (hydrological model, thermal and
107 microwave remote sensing) and the likely fulfilling of the main TC key ~~helps ensuring to fulfill a key~~
108 hypothesis ~~of TC, which is the~~ (i.e., independency between the errors of the three ~~models~~ datasets), the

109 TC approach seems suitable for quantifying the spatial distribution of the errors associated to each
110 dataset.

111 Following these considerations, ~~the~~ overall goal of this study is twofold. First, the agreement
112 between the monthly anomalies of the three ~~models-datasets~~ is evaluated, in order to identify the macro-
113 areas where a reliable monitoring of soil moisture extreme conditions can be performed according to
114 ~~these three -available-~~ datasets available globally and suitable for use in a near-real time monitoring
115 system. Second, the TC analysis is performed over those macro-areas to quantify the spatial distribution
116 of the expected random errors for each model compared to the unknown true status. Ultimate objective
117 of the error analysis reported in this study is to provide information on the accuracy of the datasets that
118 can be in order to -injected into a weighted-average develop a suitable combination-ensemble procedure
119 for a near-real time detection of the occurrence of ecosystem drought events, contributing. ~~Both goals~~
120 ~~will contribute to~~ the future development of a robust agricultural drought monitoring index within the
121 GDO system.

123 2. Methods

124
125 Drought events are commonly defined as prolonged periods during which a given drought
126 indicator significantly deviates from the usual condition for the specific site and period (e.g., soil
127 moisture content is lower than the climatology). Following this definition, this study will focus on
128 standardized z-score values in order to make the different datasets directly comparable ~~the different~~
129 ~~datasets~~ (i.e., minimizing the differences related to seasonality, soil depth, etc.). Specifically, monthly z-
130 score values, or anomalies, are evaluated as:

$$131 \quad Z_{x,i,k} = \frac{x_{i,k} - \mu_{x,i}}{\sigma_{x,i}} \quad (1)$$

132 where $x_{i,k}$ is the monthly average variable for the i -th month at the k -th year, $\mu_{x,i}$ and $\sigma_{x,i}$ are the long-
133 term average and standard deviation of the variable x for the i -th month, respectively. The baseline
134 period adopted to compute the twelve reference- μ and σ ~~twelve-monthly~~ reference values should be of

135 15-30 years in order to ensure a stable benchmark. The three datasets used here, as described in the next
136 section, are the root zone soil moisture data from the Lisflood model ($x = LIS$), the ESA [Climate](#)
137 [Change Initiative](#) skin soil moisture microwave combined product ($x = CCI$) and the thermal remote
138 sensing derived [L](#)and [S](#)urface [T](#)emperature ($x = LST$); in the case of LST data, the sign of the
139 anomalies is reversed due to the expected inverse relationship between soil moisture and LST.

140 The monthly aggregation period is chosen to ensure a statistical robustness of the computed
141 anomalies, as well as to minimize the presence of missing data in the remote sensing datasets due to
142 sub-optimal acquisition conditions (e.g., cloudy days for LST). The transition from daily data to
143 monthly aggregated values also ensures a reduction in the likely discrepancies among the three datasets
144 introduced by the differences in the explored soil depth, since the phase shift in time-aggregated
145 quantities is usually less marked (Campbell and Norman, 1998). Additionally, the time-series of
146 anomalies computed according to Eq. (1), ~~are~~ characterized by a null average and a unitary standard
147 deviation, making allow for a a direct comparison of the different datasets ~~simpler~~ thanks to the removal
148 of potential biases; ~~additionally, in the is~~ particular case of a regression analysis between two
149 standardized anomaly quantities, the Pearson correlation coefficient, R , represents not only a measure of
150 the linear dependency of the two random ~~quantities-variables~~
151 and a proxy of the difference and biases of the two datasets. In this respect, R can be seen as a good
152 synthetic descriptor of the relationship between two standardized z-score datasets. The statistical
153 significance of the existence of a positive correlation can be evaluated by means of the [Student's](#) t-
154 ~~student~~ test (2 sided) by computing the R value corresponding to a significance level $p = 0.05$.

155 Analysis of the correlation among the datasets is interesting in the framework of the triple
156 collocation (TC) technique and its basic hypotheses. In TC, a first key hypothesis is the existence of
157 linearity between the 'true' status of the system and the three models; this is formally expressed as:

$$158 \quad z_x = \alpha_x + \beta_x z_\Theta + \varepsilon_x \quad (2)$$

159 where z_Θ is the unknown true dataset of soil moisture anomalies, α_x and β_x are the systematic slope and
160 bias parameters for the dataset x with respect to the truth, and ε_x is the additive zero-mean random noise.

161 It follows that the absence of a statistical significant linear relation between all three models openly
162 violates this hypothesis.

163 Other key underling hypotheses of TC are the stationarity of both signals and errors, the
164 independency between the errors and the signal (error orthogonality) and the independence between the
165 errors of the three datasets (zero-cross correlation) (Gruber et al., 2016). Finally, operational limitations
166 regard the minimum sample size of each dataset, which is commonly assumed equal to 100 values
167 (Scipal et al., 2008; Dorigo et al., 2010), even if some other authors suggest much larger sample sizes
168 for a lower relative uncertainty (Zwieback et al., 2012).

169 Under these assumptions, Stoffelen (1998) proposed a formulation to estimate each model error
170 variance, $\sigma_{\varepsilon_x}^2$, based on a combination of the covariance between the datasets. In this approach, known
171 as the covariance notation (Gruber et al., 2016), the error variance values are computed without a
172 common (arbitrary) reference dataset as:

$$\begin{aligned} \sigma_{\varepsilon_1}^2 &= \sigma_1^2 - \frac{\sigma_{12}\sigma_{13}}{\sigma_{23}} \\ \sigma_{\varepsilon_2}^2 &= \sigma_2^2 - \frac{\sigma_{21}\sigma_{23}}{\sigma_{13}} \\ \sigma_{\varepsilon_3}^2 &= \sigma_3^2 - \frac{\sigma_{31}\sigma_{32}}{\sigma_{12}} \end{aligned} \quad (3)$$

174 where, for the sake of simplicity, LIS, LST and CCI were renamed 1, 2, 3, respectively. The first term
175 on the right side of Eqs. (3) represents the single model data variance, whereas the second term
176 represents the so-called sensitivity of the model to variations in the true status, which is a function of the
177 covariance terms between the three models. The advantage of this formulation is to directly estimate the
178 unscaled error variances, which can (eventually) be scaled to a common data space, if needed.

179 In the case of the application of the covariance notation to standardized quantities (with zero mean
180 and unitary standard deviation), the error variance values computed through Eqs. (3) are expressed as
181 dimensionless multiples of standard deviation, and a transformation to a common data space is not
182 needed.

183 Different performance metrics can be derived from the covariance notation, including relative
184 error variance metrics such as the fractional root-mean-squared-error (fRMSE, Draper et al., 2013) and
185 the correlation coefficient of each model with the underlying true signal (McColl et al., 2014).

186 However, these metrics can be derived from each other by means of simple relationships (see Gruber et
187 al., 2016) and they are analogous to the absolute error variance values in the case of z-scores values-that
188 have known unitary dataset variance.

189

190 **3. Data and Materials**

191

192 *3.1 Lisflood model soil moisture*

193

194 Root zone soil moisture dynamics are simulated by means of the Lisflood model (de Roo et al.,
195 2000), a GIS-based distributed hydrological rainfall-runoff-routing model designed to reproduce the
196 main hydrological processes that occur in large and trans-national European river catchments. The
197 model simulates all the main hydrological processes occurring in the land-atmosphere system, including
198 infiltration, actual evapotranspiration, soil water redistribution in three sub-layers (surface, root zone
199 and sub-soil), surface runoff routing to channel, and groundwater storage and transport (Burek et al.,
200 2013).

201 Static maps used by the model are related to topography (i.e., digital elevation model, local drain
202 direction, slope gradient, elevation range), land use (i.e., land use classes, forest fraction, fraction of
203 urban area), soil (i.e., soil texture classes, soil depth), and channel geometry (i.e., channel gradient,
204 Manning's roughness, bankfull channel depth, channel length, bottom width and side slope). Root zone
205 depth is defined for each modelling cell on the basis of soil type and land use, where ~~T~~the soil-related
206 hydraulic quantities-properties are obtained from the ISRIC 1-km SoilGrids database (Hengl et al.,
207 2014), whereas topography data are obtained from the Hydrosheds database (Lehner et al., 2008).

208 Daily meteorological forcing maps are derived from the European Centre for Medium-range
209 Weather Forecasts (ECMWF) data as spatially resampled and harmonized by the JRC Monitoring
210 Agricultural ResourceS (MARS) group. The dataset includes daily average air temperature, potential
211 evapotranspiration (for soil, water and reference surfaces) and total rainfall at 0.25 degree spatial
212 resolution, which were resampled on the model grid using the nearest neighbors algorithm.

213 The model run used in this study includes daily maps at 0.1 degree resolution between 1989 and
214 2015; the grid domain of this dataset is used as reference for the other two, whereas the baseline for the
215 anomalies computation is defined by the period 2001-2015 in order to match the LST data availability.
216 Monthly data to be used in Eq. (1) are computed as a simple average of all the data available for each
217 month, given that no gaps can be found in this dataset due to its continuous nature as hydrological
218 model. However, some areas were masked out due to the minimum or null temporal dynamic of soil
219 moisture, such as Greenland and the Sahara desert.

220

221 ***3.2 Land Surface Temperature dataset***

222

223 The use of the land surface temperature (LST) anomalies as a proxy of soil moisture anomalies is
224 based on the well-known role of LST in the surface energy budget as a control factor for the partitioning
225 between latent and sensible heat fluxes. In recent years, the existence of a connection between soil
226 moisture and LST has been analyzed, mainly through the thermal inertia and the triangle methods (e.g.,
227 Carlson 2007; Verstraeten et al., 2006), as well as a direct proxy (see e.g., Park et al., 2014; Srivastava
228 et al., 2016). In a study over the pan-European domain, Cammalleri and Vogt (2016) have demonstrated
229 the good agreement between monthly LST and LIS-based root zone soil moisture z-score values during
230 summer time, where LST outperforms other LST-based indicators such as the day-night difference and
231 the surface-air gradient.

232 Following these findings, this study adopts the dataset collected by the Moderate-Resolution
233 Imaging Spectroradiometer (MODIS) sensor on board of the Terra satellite
234 (<http://terra.nasa.gov/about/terra-instruments/modis>) as a source of monthly-scale long records of LST
235 maps. In particular, the MOD11C3 Monthly CMG (Climate Modelling Grid) LST product is used in
236 this study, which is constituted by monthly composited and averaged temperature and emissivity maps
237 at a spatial resolution of 0.05 degrees over a regular latitude/longitude grid; data for the period 2001–
238 2015 are used, as the only fully completed years at the time of the analysis.

239 This monthly composite product is obtained as an average of the clear-sky data in the MOD11C1
240 products on the calendar days of the specific month, which are derived after a re-projecting and a re-
241 sampling of the MOD11B1 product. Details on the algorithms used to obtain the daily MOD11B1 maps
242 can be found in Wan et al. (2002); in summary, a double screening procedure is applied, based on: i) the
243 difference between the two independent LST estimates of the day/night algorithm (Wan and Li, 1997)
244 and the generalized split-window algorithm (Wan and Dozier, 1996), and ii) the histogram of the
245 difference between daytime and nighttime LSTs.

246 LST monthly maps were spatially co-registered to the Lisflood 0.1 degree regular
247 latitude/longitude grid by means of a simple average of the values within each cell, and anomaly maps
248 were computed according to Eq. (1) by using only the data for which $LST > 1\text{ }^{\circ}\text{C}$; this threshold value
249 (commonly used in snowmelt and snow/rainfall discrimination procedures; WMO, 1986) allows
250 removing the data that are likely affected by snow/frost from the analysis.

251

252 ***3.3 Microwave combined dataset***

253

254 The ESA Climate Change Initiative (CCI) aims at developing a multi-satellite soil moisture
255 dataset by combining data collected in both past and present by passive and active microwave
256 instruments (~~Dorigo et al., 2016~~[Liu et al., 2012](#); [Wagner et al., 2012](#)). The current version of the dataset
257 ([v03.2](#)) combines data from nine different sensors (SMMR, ERS-1/2, TMI, SSM/I, AMSR-E, ASCAT,
258 WindSat, AMSR2 and SMOS) between 1978 and 2015.

259 Satellite-based microwave estimates of soil moisture are usually related to the first few
260 centimeters of soil column (i.e., skin layer), which is quite closely related to the soil moisture content in
261 the root zone (Paulik et al., 2014), except for very dry conditions [in sandy soils](#). Additionally, numerous
262 validations against land surface models have highlighted good performance across the globe, with
263 notable exceptions over densely vegetated areas (e.g., Loew et al., 2013).

264 The algorithm adopted to merge the different data sources is the one developed by Liu et al.
265 (2012), which is a three-step procedure that: i) merges the original passive microwave products, ii)

266 merges the original active microwave products, and iii) blends the two merged products into a single
267 final dataset. The merging procedure of passive datasets includes pixel-scale separation between
268 seasonality and anomalies, rescaling of the data based on the piece-wise cumulative distribution
269 function (CDF) and merging of the dataset using a common reference seasonality. For the active
270 microwave instruments, the CDFs are directly used to rescale the data under the assumption that active
271 datasets have an identical dynamic range, this mainly due to the limited overlap between datasets. The
272 final blending of the two merged datasets is obtained by adopting a common resolution of
273 approximately 25 km and daily frequency, as well as by using the GLDAS-1-Noah model
274 (<ftp://agdisc.gsfc.nasa.gov/data/s4pa/>) as a reference dataset for the CDF matching.

275 In this study, the daily blended dataset is spatially resampled to a 0.1 degree regular
276 latitude/longitude grid (the same used in Lisflood simulations) by means of the nearest neighbor
277 algorithm, and successively aggregated to monthly time scale by simply averaging the data (only if at
278 least 8 daily values were available in the specific month). Monthly average maps were converted into z-
279 score maps by using the baseline period 2001-2015 (the timeframe available for the LST dataset).

280 Monthly aggregated z-score values of skin soil moisture are analyzed, jointly with the other two
281 datasets, under the assumption that time-aggregation and normalization procedures minimize some of
282 the discrepancies that are likely present between skin and root zone daily time-series.

283

284 4. Results and Discussion

285

286 Considering the assumption of linearity between each one of the ~~models-datasets~~ and the unknown
287 true status of the system in TC, a preliminary analysis on the linear correlation between the three
288 ~~anomaly models-products~~ has been performed in order to detect the macro-areas where the TC
289 procedure can be applied without violating this basic hypothesis. The correlation analysis was
290 performed by using only the monthly ~~anomalies data~~ that were available for all three ~~models-datasets~~,
291 with at least a sample size of 100 values (max sample size = 12 months × 15 years = 180), and by

292 defining a minimum correlation threshold ($R_{0.05}$) that ensures a statistical significance of the linear
293 relationship on the basis of the Student's t-student test (at $p = 0.05$).

294 The map in Fig. 1 reports in grey the areas where all three ~~models-datasets~~ are significantly
295 linearly correlated according to the described criteria, representing the areas where the first basic
296 hypothesis of the TC is not clearly violated. It is worth to point out that some areas are excluded from
297 the analysis by the lack of data in LIS (low temporal variability, as over Greenland and the Sahara
298 desert), LST (due to the minimum temperature threshold or low temporal variability) or CCI (densely
299 vegetated areas, such as the Amazon forest and the Congo basin). These results suggest to focus the
300 successive detailed analysis on five macro-regions (demarked by the boxes in Fig. 1) that have
301 consistent positive correlation values for all the three ~~modelsdatasets~~; these areas are named, from now
302 on, as: 1) NA (including the contiguous U.S. and Mexico), 2) EU (Southern and Central Europe), 3) SA
303 (Southern countries of the African continent and Madagascar), 4) IN (Indian subcontinent), and 5) AU
304 (Australia)*.

305 The correlation coefficient maps over those regions, obtained by inter-comparing the three
306 ~~modelsdatasets~~, are reported in Figs. 2 to 4, where the cells in red and yellow are the ones with negative
307 or not-significant correlation, respectively, whereas the blue scale represents the cells with increasing
308 significant linear correlation (from light to dark tones). The comparison between LIS and LST (Fig. 2)
309 shows an overall good agreement between the two datasets, with only minor areas characterized by
310 negative/not-significant correlation values; notably, low correlation can be observed over the Great
311 Lakes and Rocky mountain areas in the U.S., over the Alps in Europe, North Angola and Western
312 Himalaya. Similar results can be observed in Fig. 3, where LIS and CCI datasets are compared; this
313 comparison shows an increasing number of negative values in the Western U.S., the Alps, and Southern
314 Turkey, but overall high correlation values across most of the five regions. Finally, the comparison
315 between LST and CCI reported in Fig. 4 shows an increase of areas with low/not-significant correlation
316 in the Eastern and Western U.S. and both North- and South-Eastern Europe and the Alps, whereas a
317 high correlation can be observed all over the other regions.

* Consider the countries and boundaries reported here only as indicative of the interested areas, and they may not in any circumstances be regarded as stating an official position of the European Commission.

318 On average, the data in Table 1 summarize the results obtained for all the regions together, as well
319 as for each region independently, showing how CCI and LST are the two datasets best correlated to
320 each other overall, even if this result is mainly driven by the results over AU, SA and IN macro-areas.
321 The data of the LIS model are similarly correlated to the ones of LST and CCI, with a more uniform
322 distribution of the results across the various sub-regions. Another outcome of this analysis is that the
323 area with the lowest average correlation between the three ~~models-datasets~~ is [the](#) EU, probably due to
324 the high heterogeneity of this region at the 0.1 degree spatial scale.

325 Some of the discrepancies observed in Figs. 2 to 4 can be explained by the differences in both
326 horizontal and vertical resolution of the three raw datasets. LIS is characterized by an higher spatial
327 resolution (5-km) compared to CCI (25-km) and a vertical resolution that encompasses the full root
328 zone against the skin soil moisture of the latter; LST has the same spatial resolution of LIS but a vertical
329 resolution that varies as function of the vegetation coverage between skin (for bare soil) to root zone
330 (for full [vegetation](#) coverage). The impact of such- differences is partially reflected in the observed
331 results, with CCI-LST better related over shallow soil in homogeneous areas, and LIS-LST better in
332 agreement over sparse agricultural areas in Europe. Overall, it seems that the adopted expedients (i.e.,
333 monthly average, standardization) successfully minimized these issues, given that the results in Table 1
334 shows a substantial [and](#) similar agreement of the three datasets in the main areas.

335 ~~Overall~~Additionally, the obtained results seem to suggest that [it is reliable to adopt use-of](#) LST
336 anomalies as proxy of soil moisture anomalies ~~seems based on a reliable assumption~~, since there is a
337 clear consistency of LST anomalies with the other two datasets. Similar results were obtained by Fang
338 et al. (2016) over [the](#) ~~€~~continental United States, where the outputs of the thermal-based ALEXI
339 (Atmosphere Land EXchange Inverse) model compares well with soil moisture anomalies from CCI
340 and Noah land-surface model. This consideration allows applying the TC analysis to the LST dataset as
341 well, whereas most of the studies in the literature focus on land modelled and microwave soil moisture
342 datasets (i.e., Dorigo et al., 2010; Gruber et al., 2016; Su et al., 2014) with only few notable exceptions
343 including thermal data (e.g., Hain et al., 2011; [Yilmaz et al., 2012](#)).

344 The outputs of the correlation analysis were used to detect the cells suitable for the TC technique;
345 since a key hypothesis of the technique is the existence of a linear relation between each model and the
346 (unknown) truth, a necessary condition (even if not sufficient) is the existence of linear relationships
347 among the three models/datasets. As outcome of the correlation analysis, around 10% of the five macro-
348 areas were removed from the TC analysis due to the absence of this basic condition.

349 The maps in Figs. 5 to 7 show the main outcome of the TC analysis, which is the spatial
350 distribution of the error variance (dimensionless, as showing the multiple of model standard deviation)
351 for each model, as detailed by Eqs. (3). The blank areas in those maps correspond to the cells where no
352 significant linear correlation was observed between all three models/datasets. The results for LIS (Fig. 5)
353 show how the highest errors are observed over the Western U.S., Northern Cape in South Africa and
354 Western/Southern Australia, whereas low errors are observed over the Eastern U.S. On the opposite, the
355 LST dataset displays the highest errors over the latter area (Fig. 6), whereas the lowest errors are
356 observed over Queensland in Australia, Eastern Cape in South Africa and Lesotho. The maps in Fig. 7
357 show that the CCI dataset has consistent patterns of low error variance values over most of Australia,
358 Western India and Central U.S.

359 Overall, on the one hand, it seems evident how CCI tends to outperform the other two methods
360 over dry areas such as Australia and South Africa, but on the other hand, a region like the U.S. is almost
361 equally subdivided among the three models/datasets, where LIS performs better in the East, LST in the
362 West and CCI in the center. Differences among models-products can be partially explained by the
363 differences in the soil layer monitored by each dataset, i.e., microwave system capturing skin soil
364 moisture whereas Lisflood models the full root zone; indeed, even if the use of monthly anomalies
365 allows minimizing some of the discrepancies, skin soil moisture remains more reliable for dry/bare
366 areas (Das et al., 2015). Even if these considerations partially explain the agreement/disagreement
367 behavior of the three datasets, it is not straightforward to pinpoint in details climate and/or vegetation
368 derived patterns in the spatial distribution of the TC outputs.

369 These findings are summarized in the data reported in Table 2, where the average error variance
370 for each model and macro-area is reported aside its spatial standard deviation. The data in Table 2

371 confirm that CCI has an overall better performance (lower errors) than LIS and LST, which perform
372 quite closely, mainly thanks to the very low error variance observed over Australia and, to a minor
373 extend, Southern Africa. The LIS model shows to perform better over NA and EU regions, likely due to
374 the better meteorological forcing datasets available over those regions compared to the other macro-
375 areas (due to denser ground networks). The LST dataset seems to perform moderately well over all five
376 macro-regions, with the only notable exception of EU; however, it rarely outperforms the other two
377 datasets, constituting a “second-best” option in most of the cases. It is also worth to point out that the
378 CCI dataset is often masked-out over those regions where the error of microwave techniques are likely
379 high, whereas the data of the other two datasets are mostly produced globally; hence, a possible
380 explanation of the better performance of CCI compared to LIS and LST may be linked to this
381 preliminary screening of the data.

382 The outcome that LIS slightly outperforms the other two datasets over NA is in agreement with
383 the results reported by Hain et al. (2011), where the Noah land-surface model slightly outperforms (on
384 average) the microwave and thermal datasets over Contiguous U.S. However, it should be pointed out
385 how the spatial distribution of the error estimates for LIS differs from the ones reported for Noah, likely
386 due to the differences in both meteorological forcing and modelling approaches. Some qualitative
387 analogies can be also be observed with the results reported in Similarly, Pierdicca et al. (2015), which
388 shows smaller average errors at daily time scale over Europe for the ERA-LAND modelled datasets
389 compared to two microwave-based datasets, even if both the temporal scale and the adopted
390 methodology of the latter differ from the ones used in similarly to the results obtained in this our study.
391 ~~Both of these previous study results~~ seems to ~~suggest confirm~~ that land modelling approaches are more
392 reliable, on average, over these regions, likely due to the reliability of meteorological forcing and model
393 parameterizations, even if there can be significant differences among the performances of different
394 land-surface models.

395 Over AU sub-region, the spatial distribution of the errors in CCI are quite in agreement with the
396 results reported in Su et al. (2014) for two microwave datasets, with larger errors along the South-East
397 Australian coast. This result supports the assumption that microwave data are more reliable over dry

398 bare soil areas, which is further highlighted by the results obtained in SA and IN sub-regions. The
399 subdivision of the NA domain in three main regions is similar to the one observed by Gruber et al.
400 (2016) in comparing ASCAT and AMSR-E microwave datasets, suggesting key differences in the soil
401 moisture behavior over these three sub-regions. Overall, the spatial patterns of microwave and land
402 model errors show similarities with the ones observed by Dorigo et al. (2010), even if no thermal data
403 were included in their analysis.

404 The error variance values can also be interpreted as the correlation coefficient of each dataset with
405 the underlying true signal, following the definition of McColl et al. (2014). In fact, for the special case
406 of anomalies with unitary variance ($\sigma_x^2 = 1$), the TC-derived R_x of each dataset is simply equal to
407 $\sqrt{1 - \sigma_{\varepsilon_x}^2}$, which ranges on average over all five regions (not shown) between 0.91 (for CCI in AU) to
408 0.66 (for LST over EU); these values show a good capability of the models-datasets to capture, on
409 average, temporal variations in soil moisture anomalies.

410 In order to provide a simple synthetic representation of the likely best model for each area, the
411 map in Fig. 8 depicts for each cell the dataset with the lowest error variance by associating different
412 colors to the three models-datasets (red for LIS, blue for LST and green for CCI). Even if this approach
413 is rather simplistic, as it cannot account for two models-products performing really close over some
414 areas, the major relevant features, like the predominance of the CCI model over Australia, are made
415 evident by these maps.

416 The maps in Fig. 8 confirm CCI as the dataset with the lowest error variance values over most of
417 AU, SA and IN, whereas the three models-datasets almost equally split the other two macro-areas; this
418 is even more evident in the data reported in Table 3, where the percentage of sub-areas where each
419 model is the best is reported. These data confirm the good performance of CCI over AU, SA and IN
420 macro-regions, whereas the NA territory is almost equally divided among the three datasets and LIS
421 outperforms both LST and CCI over 50% of EU domain. In the latter, the areas where the LIS dataset
422 outperforms the other two datasets partially resemble the results obtained by Pierdicca et al. (2011) for
423 the ERA-LAND model; however, the present study includes also remote sensing thermal data and not

424 only microwave-derived datasets. Overall, the CCI dataset outperforms the other two datasets in about
425 50% of cells, with the remaining almost equally split between LIS and LST.

426 Finally, the spatial distribution of the weighting factor of each dataset, computed according to the
427 least square theory (Yilmaz et al., 2012), is represented in Figs. 9 to 11. The color scale of the figures
428 was designed to represent in a neutral color the cells that have a weighting factor close to the one for a
429 simple-average (1/3), in green scale the weights greater than a simple-average (larger contribute) and in
430 orange the weights lower than the simple-average (smaller contribute). The visual intercomparison of
431 the three maps further emphasizes the good performance of the CCI product over AU and SA, the best
432 performance of LIS over the Eastern US and EU, and the good results obtained for LST in Western US
433 and Northern AU. It is worth noticing that the use of a weighted average based on the TC error
434 analysis does not seem to bring advantages over large areas of central US, EU and Eastern IN where the
435 weighting factors are close to the ones for a simple arithmetic average.

436 The behavior of the weighting factors over the five macro-areas can be synthesized by the
437 frequency diagram in Fig. 12. This plot shows the high fraction of weighting factors > 0.4 for the CCI
438 dataset, representing a predominant contribution on the ensemble mean of this product over the others,
439 whereas LST has a peak of frequency center around 1/3 (arithmetic average) and LIS has a hint of bi-
440 modal distribution. These data, together with the map in Fig. 8, confirm the fact that CCI outperforms
441 the other two datasets in 50% of the domain, whereas LST is often the second-best option behind either
442 CCI or LIS.

443

444 **5. Summary and Conclusions**

445

446 Three datasets have been compared as proxy of the unknown true status of soil moisture
447 anomalies in the context of the global drought monitoring system under development by the JRC of the
448 European Commission. Key assumption of the study is the inability of a single dataset to accurately
449 capture the soil moisture dynamic over the large range of variability of conditions that can be observed
450 at continental to global scale.

451 The inter-comparison between the three datasets, namely the outputs of the Lisflood hydrological
452 model (LIS), the MODIS-based land surface temperature (LST) and the combined active/passive
453 satellite microwave (CCI) data, confirms some inconsistencies between the three datasets over some
454 certain areas, as well as the difficulties in comparing the three datasets over peculiar areas (e.g., Sahara
455 desert, Amazon rainforest) due to the lack of coverage from one or more datasets. Generally, the three
456 datasets seem comparable over most of the globe, thanks to the use of time-aggregation and
457 standardization procedures that remove temporal inconsistencies and biases among the series. Focusing
458 the analysis only on the areas where the three models-datasets are substantially in agreement (following
459 a linear regression analysis), five macro-regions were detected as suitable for further investigations
460 according to the Triple Collocation (TC) technique. This analysis allows quantifying the likely random
461 error associated with each model (with regard to the true status) even in absence of an observation of
462 the “truth”, under the hypothesis that certain criteria are met.

463 The main outcome of the TC analysis further confirms the need of a multi-source approach for a
464 reliable assessment of soil moisture anomalies over those five regions, given that no model outperforms
465 the others (in terms of expected error variance) for the entire study domain. Emblematic are the results
466 over North America, where each model outperforms the others in one sub-region, like the LIS approach
467 in Eastern U.S., LST in the Southern-Western domain and CCI in Central U.S. Even if no clear insight
468 on the general patterns of the errors can be provided as outcome of the study, Overall, the obtained
469 results seem suggesting that remote sensing datasets ~~seem to~~ perform better over dry areas and sparsely
470 monitored areas (e.g., Australia and Southern Africa), whereas the LIS dataset seems more reliable over
471 NA and EU where dense networks of meteorological ground stations are deployed.

472 It has been highlighted how some differences among models-the datasets can also be related to the
473 depth of the soil layer monitored by each dataset, i.e., the microwave system capturing skin soil
474 moisture whereas Lisflood models the full root zone; indeed, even if the use of monthly anomalies
475 allows minimizing some of the discrepancies and biases, our results confirm that skin soil moisture
476 remains more reliable for ~~dry/bare~~ areas where the effects of vegetation coverage is minimal (Das et al.,
477 2015), whereas hydrological models are more suited for agricultural and densely vegetated regions.

478 However, the three datasets seems to be overall comparable in terms of average performances,
479 supporting the success of the adopted homogenization procedures. Some analogies between the
480 obtained results and the ones already available in the literature have been found, but the inclusion of
481 thermal data into the analysis enlarges the understanding of the mutual relationship between the
482 different datasets.

483 The results of this study represent a robust starting point for the development of a global drought
484 monitoring system based on such anomaly datasets, which can exploit the main findings of the TC
485 analysis in order to develop a suitable ensemble product over the investigated regions. The error
486 characterization derived from TC was used to estimate the weighing factors of an ensemble mean
487 procedure, based on the least squares framework reported in Yilmaz et al. (2012). Currently, an
488 operational implementation of such ensemble product is foreseen for the GDO system as soon as the
489 CCI product becomes available in near-real time.

490 Further analyses are required to be able to extend the test to the areas currently not included in this
491 study, especially the ones where the three datasets are available but provide inconsistent or contrasting
492 results. In this context, the analysis of further global datasets may help in unveil the reasons behind such
493 discrepancies.

494

495 **References**

496

497 Anderson, M.C., Norman, J.M., Mecikalski, J.R., Otkin, J.P., Kustas, W.P., 2007. A climatological
498 study of evapotranspiration and moisture stress across the continental U.S. based on thermal
499 remote sensing: II. Surface moisture climatology. *J. Geophys. Res.* 112, D11112,
500 doi:10.1029/2006JD007507.

501 Burek, P., van der Knijff, J.M., de Roo, A., 2013. LISFLOOD: Distributed Water Balance and Flood
502 Simulation Model. JRC Scientific and Technical Reports, EUR 26162 EN, 142 pp.
503 doi:10.2788/24719.

504 Cammalleri, C., Vogt, J.V., 2016. On the role of Land Surface Temperature as proxy of soil moisture
505 status for drought monitoring in Europe. *Remote Sens.* 7, 16849-16864.

506 Cammalleri, C., Micale, F., Vogt, J.V., 2015. On the value of combining different modelled soil
507 moisture products for European drought monitoring. *J. Hydrol.* 525, 547-558.

508 [Campbell, G.S., Norman, J.M., 1998. An introduction to environmental biophysics, Springer-Verlag.,](#)
509 [New York \(NY\), USA. doi: 10.1007/978-1-4612-1626-1.](#)

510 Carlson, T., 2007. An overview of the “Triangle Method” for estimating surface evapotranspiration and
511 soil moisture from satellite imagery. *Sensors* 7(8), 1612-1629.

512 Crow, W.T., Kumar, S.V., Bolten, J.D., 2012. On the utility of land surface models for agricultural
513 drought monitoring. *Hydrol. Earth Syst. Sci.* 16, 3451-3460.

514 Dai, A., 2011. Drought under global warming: A review. *Wiley Interdiscip. Rev. Clim. Change* 2, 45-
515 65.

516 Das, K., Paul, P.K., [Dobesova, Z.](#), 2015. Present status of soil moisture estimation by microwave
517 remote sensing. *Cogent Geoscience* 1, 1084669.

518 de Roo, A., Wesseling, C., van Deusen, W., 2000. Physically based river basin modelling within a GIS:
519 The LISFLOOD model. *Hydrol. Process.* 14, 1981-1992.

520 Dirmeyer, P.A., Gao, X., Zhao, M., Guo, Z., Oki, T., Hanasaki, N., 2006. GSWP-2: multimodel analysis
521 and implications for our perception of the land surface. *Bull. Amer. Meteor. Soc.* 87, 1381–1397.

522 Dorigo, W.A., Scipal, K., Parinussa, R.M., Liu, Y.Y., Wagner, W., de Jeu, R.A.M., Naeimi, V., 2010.
523 Error characterisation of global active and passive microwave soil moisture datasets. *Hydrol.*
524 *Earth Syst. Sci.* 14, 2605-2616.

525 ~~Dorigo, W.A., Chung, D., Gruber, A., Hahn, S., Mistelbauer, T., Parinussa, R.M., Paulik, C., Reimer,~~
526 ~~C., van der Schalie, R., de Jeu, R.A.M., Wagner, W., 2016. Soil moisture [in “State of the Climate~~
527 ~~in 2015]. *Bull. Amer. Meteor. Soc.*, 97(8), S31-S32.~~

528 Draper, C., Reichle, R., de Jeu, R., Naeimi, V., Parinussa, R., Wagner, W., 2013. Estimating root mean
529 square errors in remotely sensed soil moisture over continental scale domains. *Remote Sens.*
530 *Environ.* 137, 288-298.

531 Fang, L., Hain, C.R., Zhan, X., Anderson, M.C., 2016. An inter-comparison of soil moisture data
532 products from satellite remote sensing and a land surface model. *Int. J. Appl. Earth Obs. Geoinf.*
533 48, 37-50.

534 Gruber, A., Su, C.-H., Zwieback, S., Crow, W., Dorigo, W., Wagner, W., 2016. Recent advances in
535 (soil moisture) triple collocation analysis. *Int. J. Appl. Earth Obs. Geoinf.* 45, 200-211.

536 Hain, C.R., Crow, W.T., Mecikalski, J.R., Anderson, M.C., Holmes, T., 2011. An intercomparison of
537 available soil moisture estimates from thermal infrared and passive microwave remote sensing
538 and land surface modeling. *J. Geophys. Res.* 116, D15107.

539 Hengl, T., de Jesus, J.M., MacMillan, R.A., Batjes, N.H., Heuvelink, G.B.M., Ribeiro, E., et al., 2014.
540 SoilGrids1km — Global Soil Information Based on Automated Mapping. *PLoS ONE* 9(8),
541 e105992.

542 Houborg, R., Rodell, M., Li, B., Reichle, R., Zaitchik, B., 2012. Drought indicators based on model
543 assimilated GRACE terrestrial water storage observations. *Wat. Resour. Res.* 48, W07525.
544 doi:10.1029/2011WR011291.

545 Jackson, T.J., 2006. Estimation of Surface Soil Moisture Using Microwave Sensors. *Encyclopedia of*
546 *Hydrological Sciences*, Part 5: Remote Sensing. doi: 10.1002/0470848944.hsa060.

547 Lehner, B., Verdin, K., Jarvis, A., 2008. New global hydrography derived from spaceborne elevation
548 data, *Eos* 89(10), 93–94.

549 Liu, Y.Y., Dorigo, W.A., Parinussa, R.M., de Jeu, R.A.M., Wagner, W., McCabe, M.F., Evans, J.P., van
550 Dijk, A.I.J.M., 2012. Trend-preserving blending of passive and active microwave soil moisture
551 retrievals. *Remote Sens. Environ.* 123, 280-297.

552 Loew, A., Stacke, T., Dorigo, W., de Jeu, R., Hagemann, S., 2013. Potential and limitations of
553 multidecadal satellite soil moisture observations for selected climate model evaluation studies.
554 *Hydrol. Earth Syst. Sci.* 17, 3523-3542.

555 McColl, K.A., Vogelzang, J., Konings, A.G., Entekhabi, D., Piles, M., Stoffelen, A., 2014. Extended
556 triple collocation: Estimating errors and correlation coefficients with respect to an unknown
557 target. *Geophys. Res. Lett.* 41, 6229-6236.

558 Miralles, D.G., Crow, W.T., Cosh, M.H., 2010. Estimating spatial sampling errors in coarse-scale soil
559 moisture estimates derived from point-scale observations. *J. Hydrometeorol.* 11, 1423-1429.

560 Mo, K.C., Long, L.N., Xia, Y., Yang, S.K., Schemm, J.E., Ek, M.B., 2010. Drought indices based on
561 the Climate Forecast System Reanalysis and ensemble NLDAS. *J. Hydrometeorol.* 12, 185-210.

562 Park, J.-Y., Ahn, S.-R., Hwang, S.-J., Jang, C.-H., Park, G.-A., Kim, S.-J., 2014. *Paddy Water Environ.*
563 12(1), 77-88.

564 Paulik, C., Dorigo, W., Wagner, W., Kidd, R., 2014. Validation of the ASCAT Soil Water Index using
565 in situ data from the International Soil Moisture Network. *Int. J. Appl. Earth Obs. Geoinfo.* 30, 1-
566 8.

567 Pierdicca, N., Fascetti, F., Pulvirenti, L., Crapolicchio, R., Muñoz-Sabater, J., 2015. Analysis of
568 ASCAT, SMOS, in-situ and land model soil moisture as a regionalized variable over Europe and
569 North Africa. *Remote Sens. Environ.* 170, 280-289.

570 Price, J.C., 1980. The potential of remotely sensed thermal infrared data to infer surface soil moisture
571 and evaporation. *Water Resour. Res.* 16(4), 787-795.

572 [Scipal, K., Holmes, T., de jeu, R., Naemi, V., Wagner, W., 2008. A possible solution for the problem of](#)
573 [estimating the error structure of global soil moisture datasets. *Geophys. Res. Lett.* 35, L24404.](#)
574 [doi:10.1029/2008GL035599.](#)

- 575 Sheffield, J., Goteti, G., Wen, F., Wood, E.F., 2004. A simulated soil moisture based drought analysis
576 for the United States. *J. Geophys. Res.* 109, D24108. doi:10.1029/2004JD005182.
- 577 Stoffelen, A., 1998. Toward the true near-surface wind speed: Error modelling and calibration using
578 triple collocation. *J. Geophys. Res.* 103, 7755-7766.
- 579 Srivastava, P.K., Islam, T., Singh, S.K., Gupta, M., Petropoulos, G.P., Gupta, D.K., Wan Jaafar, W.Z.,
580 Prasad, R., 2016. Soil moisture deficit estimation through SMOS soil moisture and MODIS land
581 surface temperature. In: *Satellite Soil Moisture Retrieval: Techniques and Applications*, P.K.
582 Srivastava, G.P. Petropoulos, Y.H. Kerr (Eds.), Elsevier B.V.
- 583 Su, C.-H., Ryu, D., Crow, W.T., Western, A.W., 2014. Beyond triple collocation: Applications to soil
584 moisture monitoring. *J. Geophys. Res. Atmos.* 119, 6419-6439.
- 585 Verstraeten, W.W., Veroustraete, F., van der Sande, C.J., Grootaers, I., Feyen, J., 2006. Soil moisture
586 retrieval using thermal inertia, determined with visible and thermal spaceborne data, validated for
587 European forests. *Remote Sens. Environ.* 101(3), 299-314.
- 588 [Wagner, W., Dorigo, W., de Jeu, R., Fernandez, D., Benveniste, J., Haas, E., Ertl, M., 2012. Fusion of](#)
589 [active and passive microwave observations to create an essential Climate Variable data record on](#)
590 [soil moisture. ISPRS Annal of the Photogrammetry, Remote Sensing and Spatial Information](#)
591 [Sciences, volume I-7. XXII ISPRS Congress, 25 August – 01 September 2012, Melbourne,](#)
592 [Australia.](#)
- 593 Wan, Z., Zhang, Y., Zhang, Q., Li, Z.-L., 2002. Validation of the land-surface temperature products
594 retrieved from Terra Moderate Resolution Imaging Spectroradiometer data. *Remote Sens.*
595 *Environ.* 83, 163-180.
- 596 Wan, Z., Li, Z.-L., 1997. A physics-based algorithm for retrieving land-surface emissivity and
597 temperature from EOS/MODIS data. *IEEE Trans. Geosci. Remote Sens.* 35, 980-996.
- 598 Wan, Z., Dozier, J., 1996. A generalized split-window algorithm for retrieving land surface temperature
599 from space. *IEEE Trans. Geosci. Remote Sens.* 34, 892-905.
- 600 Wilhite, D.A., 2000. Drought as a natural hazard: Concepts and definitions. N: *Disasters series.*
601 Routledge Publishers, UK, 213-230.

602 World Meteorological Organization, 1986. Intercomparison of models of snowmelt runoff. Operational
603 Hydrological Report, 23.

604 Yilmaz, M.T., Crow, W.T., Anderson, M.C., Hain, C.R., 2012. An objective methodology for merging
605 satellite- and model-based soil moisture products. Water Resour. Res. 48(11), W11502.
606 doi:10.1029/2011WR011682, 2012.

607 Yilmaz, M.T., Crow, W.T., 2014. Evaluation of assumptions in soil moisture triple collocation analysis.
608 J. Hydrometeorol. 15, 1293-1302.

609 Zwieback, S., Scipal, K., Dorigo, W., Wagner, W., 2012. Structural and statistical properties of the
610 collocation technique for error characterization. Nonlin. Processes Geophys. 19, 69-80.

611 **Tables**

612

613 **Table 1.** Summary of the Pearson correlation coefficient values (average \pm standard deviation) observed
 614 for all the regions.

Comparison	ALL	NA	EU	SA	IN	AU
LIS vs. LST	0.44 ± 0.09	0.41 ± 0.08	0.39 ± 0.07	0.48 ± 0.09	0.44 ± 0.07	0.50 ± 0.10
LIS vs. CCI	0.49 ± 0.10	0.47 ± 0.09	0.42 ± 0.08	0.48 ± 0.10	0.48 ± 0.08	0.58 ± 0.11
CCI vs. LST	0.56 ± 0.13	0.49 ± 0.14	0.37 ± 0.09	0.63 ± 0.09	0.52 ± 0.10	0.68 ± 0.07

615

616

617 **Table 2.** Summary of the TC error variance analysis, reporting the spatial average (\pm standard
 618 deviation) values observed over each macro-region.

Model	ALL	NA	EU	SA	IN	AU
LIS	0.48 ± 0.13	0.42 ± 0.14	0.44 ± 0.12	0.54 ± 0.11	0.49 ± 0.10	0.54 ± 0.14
LST	0.44 ± 0.13	0.46 ± 0.15	0.56 ± 0.10	0.37 ± 0.10	0.48 ± 0.09	0.38 ± 0.11
CCI	0.36 ± 0.18	0.46 ± 0.16	0.54 ± 0.12	0.30 ± 0.14	0.38 ± 0.16	0.17 ± 0.10

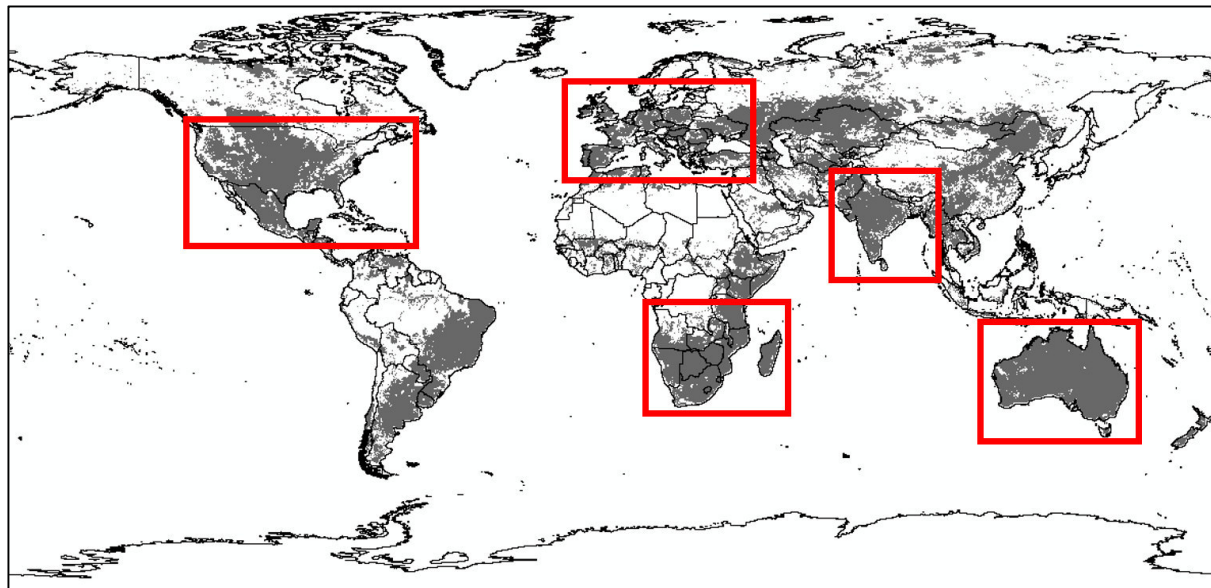
619

620

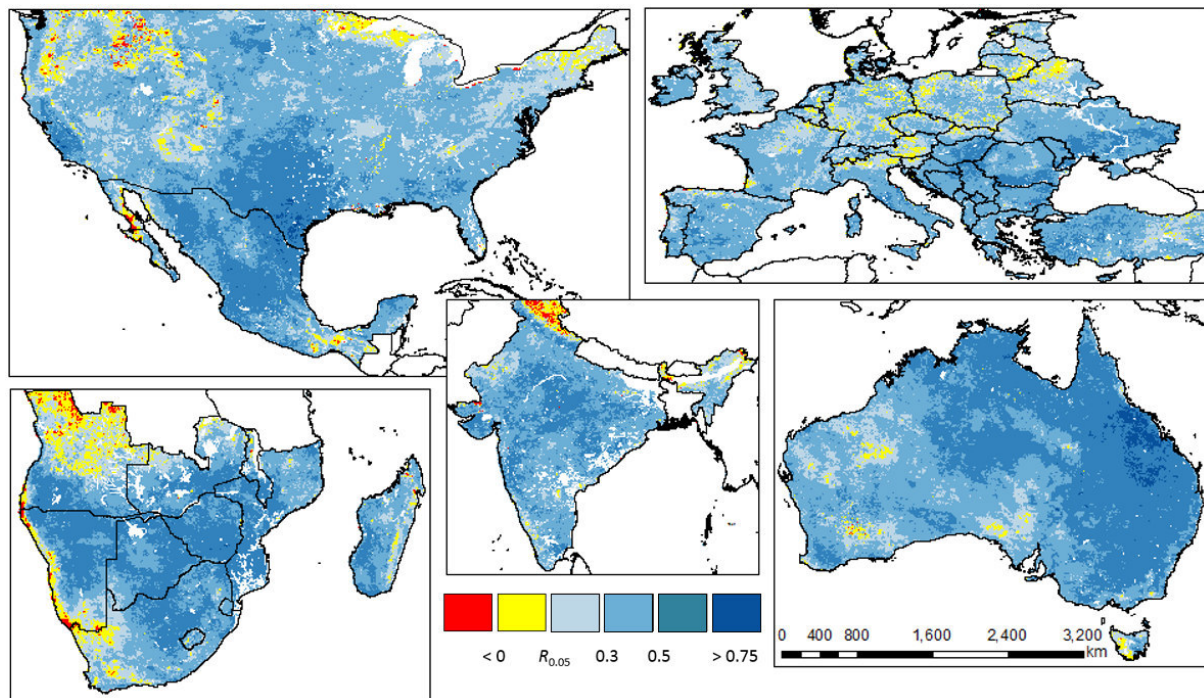
621 **Table 3.** Fraction of each macro-area (as percentage) where one model outperforms the other two.

Model	ALL	NA	EU	SA	IN	AU
LIS	25.5	39.2	50.0	10.6	28.2	4.3
LST	25.7	28.8	23.1	36.0	20.3	18.6
CCI	48.8	32.0	26.9	53.4	51.5	77.1

622

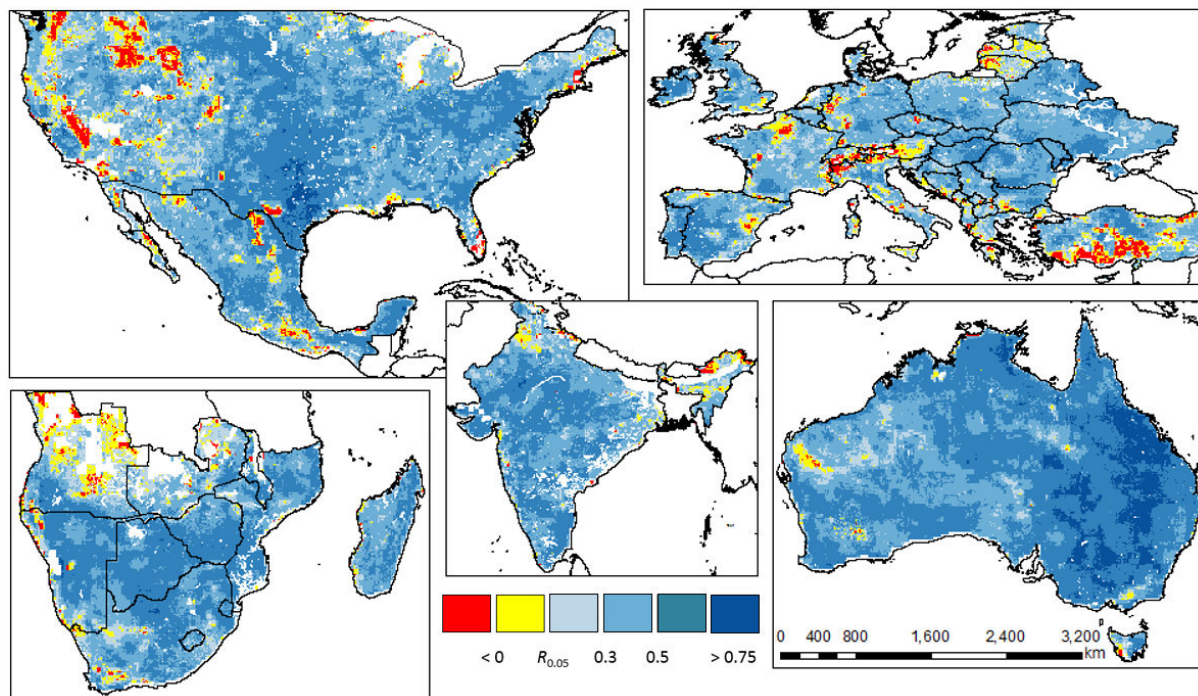


626 **Fig. 1.** Map of the areas where all the three models are positively significantly linearly correlated (cells
627 in grey) according to the Student's t-test at $p = 0.05$. The boxes delimitate the macro-regions
628 selected for the successive analyses.



630
 631 **Fig. 2.** Spatial distribution of the Pearson correlation coefficient (R) between Lisflood soil moisture
 632 anomalies (LIS) and land surface temperature anomalies (LST) over the five selected macro-regions.
 633 Values in red and yellow are negatively correlated or not significant at $p = 0.05$, respectively.

634



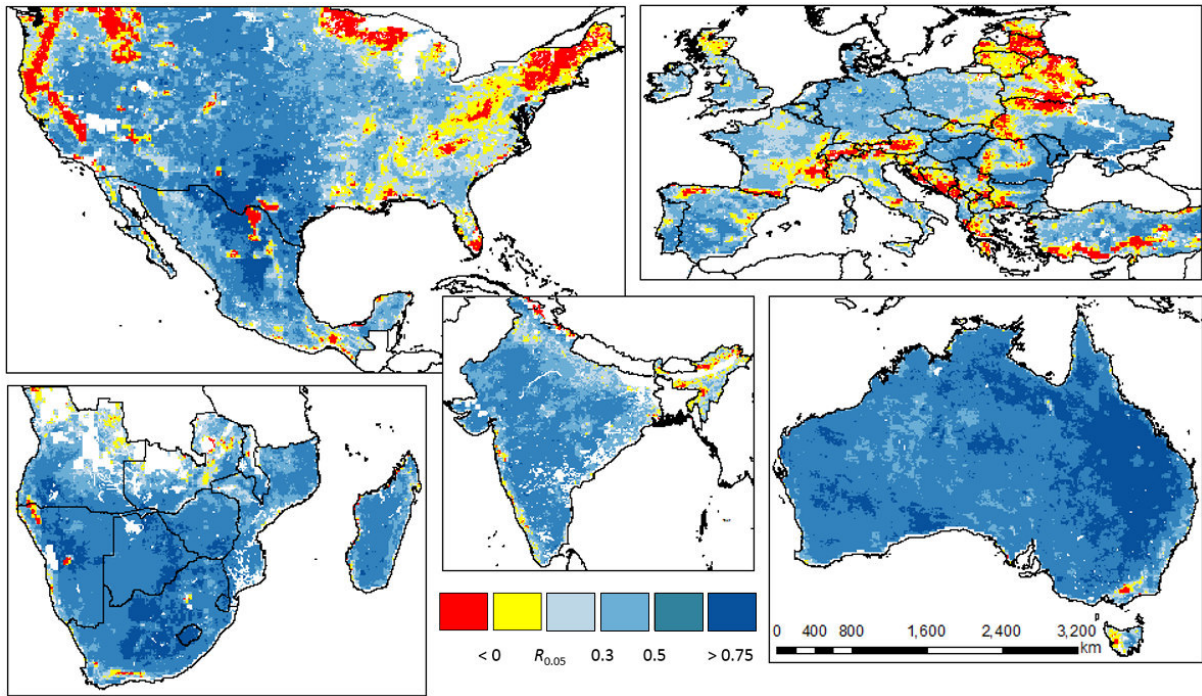
635

636 **Fig. 3.** Spatial distribution of the Pearson correlation coefficient (R) between Lisflood (LIS) and ESA

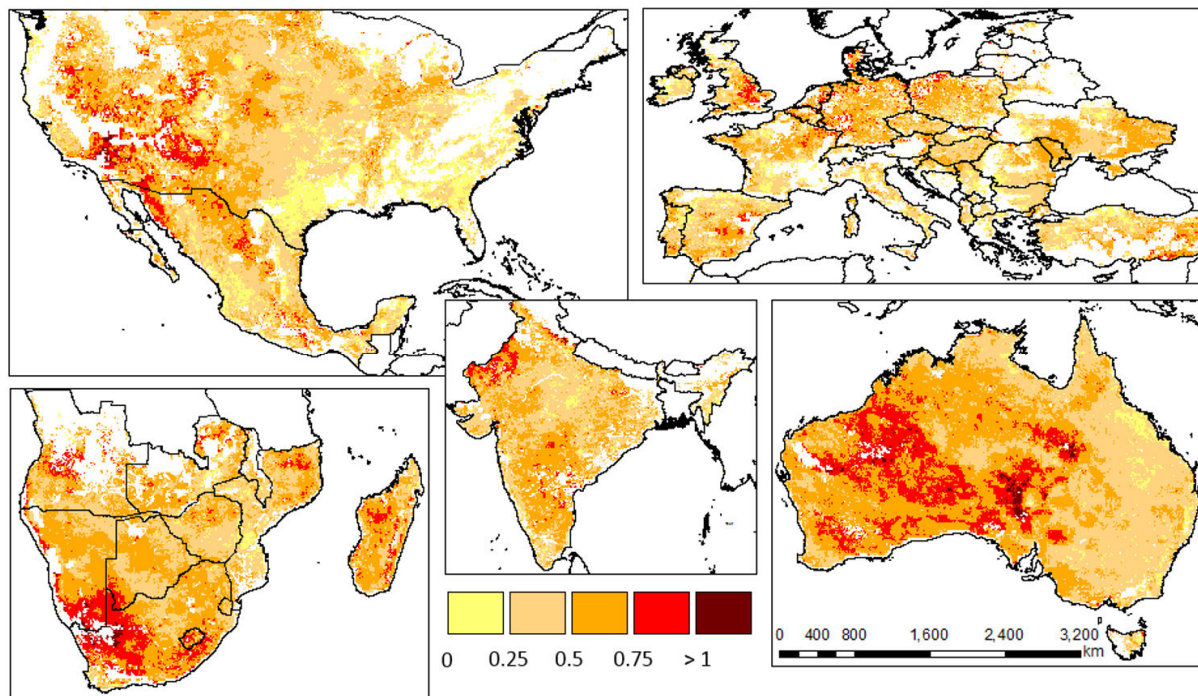
637 Climate Change Initiative (CCI) soil moisture anomalies over the five selected macro-regions. Values in

638 red and yellow are negatively correlated or not significant at $p = 0.05$, respectively.

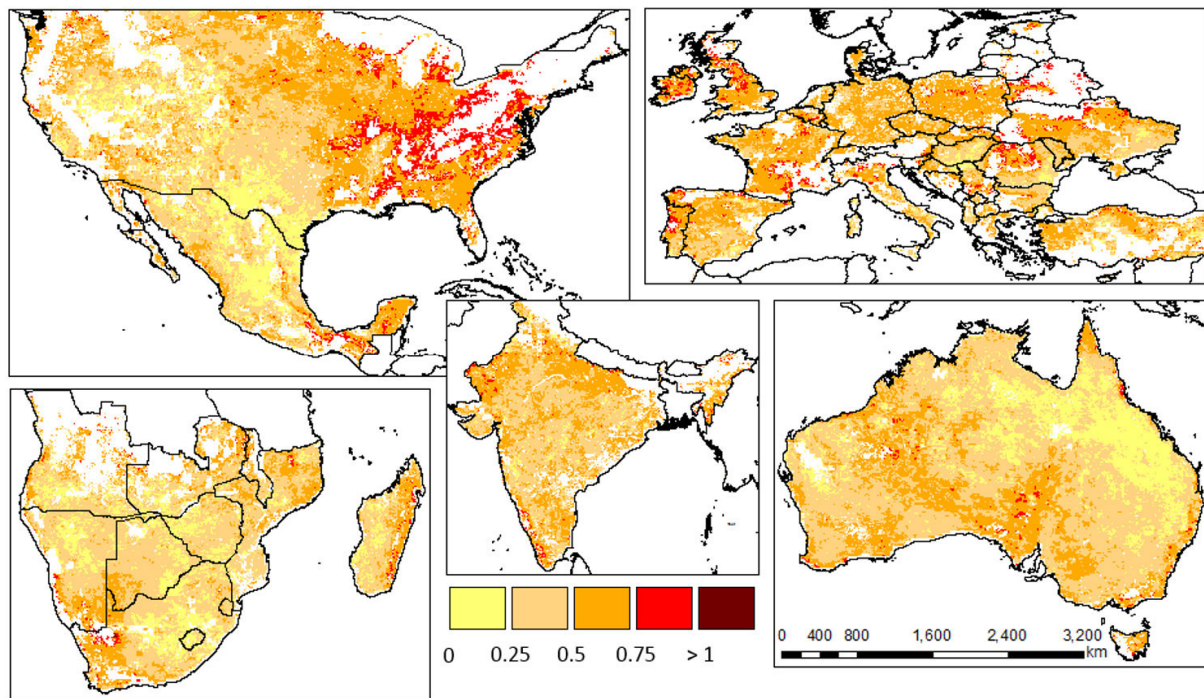
639



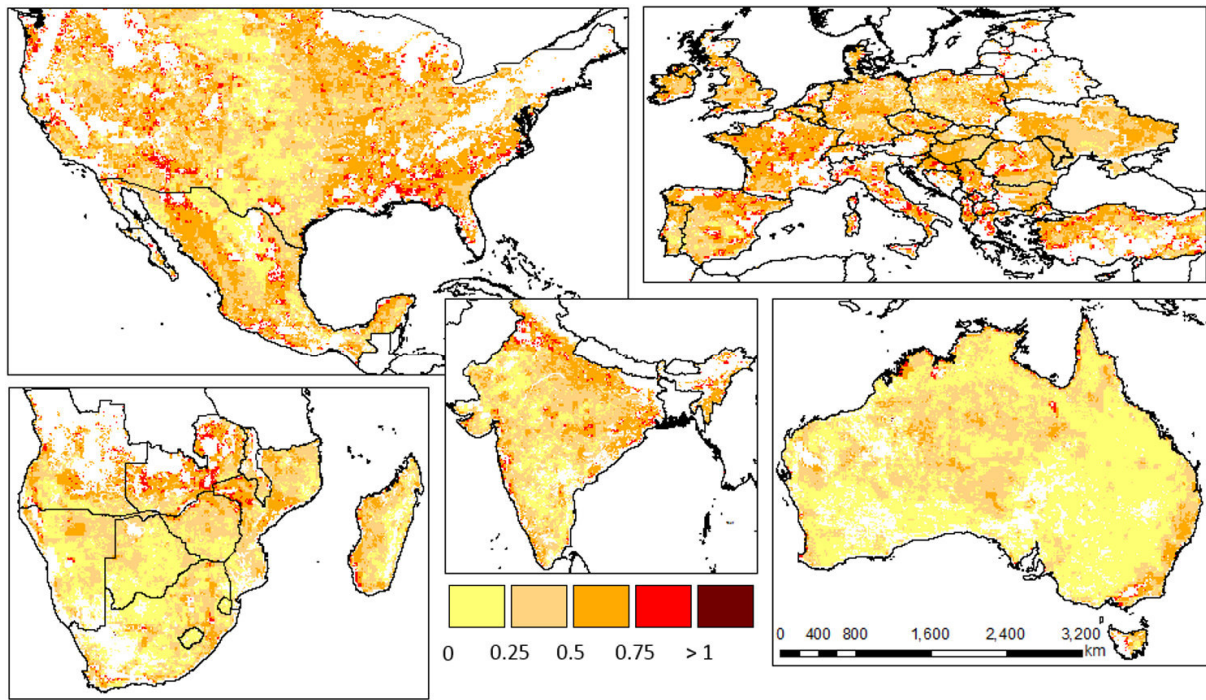
640
 641 **Fig. 4.** Spatial distribution of the Pearson correlation coefficient (R) between ESA Climate Change
 642 Initiative soil moisture anomalies (CCI) and land surface temperature anomalies (LST) over the five
 643 selected macro-regions. Values in red and yellow are negatively correlated or not significant at $p = 0.05$,
 644 respectively.
 645



646
 647 **Fig. 5.** Spatial distribution of the error variance for the Lisflood (LIS) dataset over the five selected
 648 macro-regions.
 649

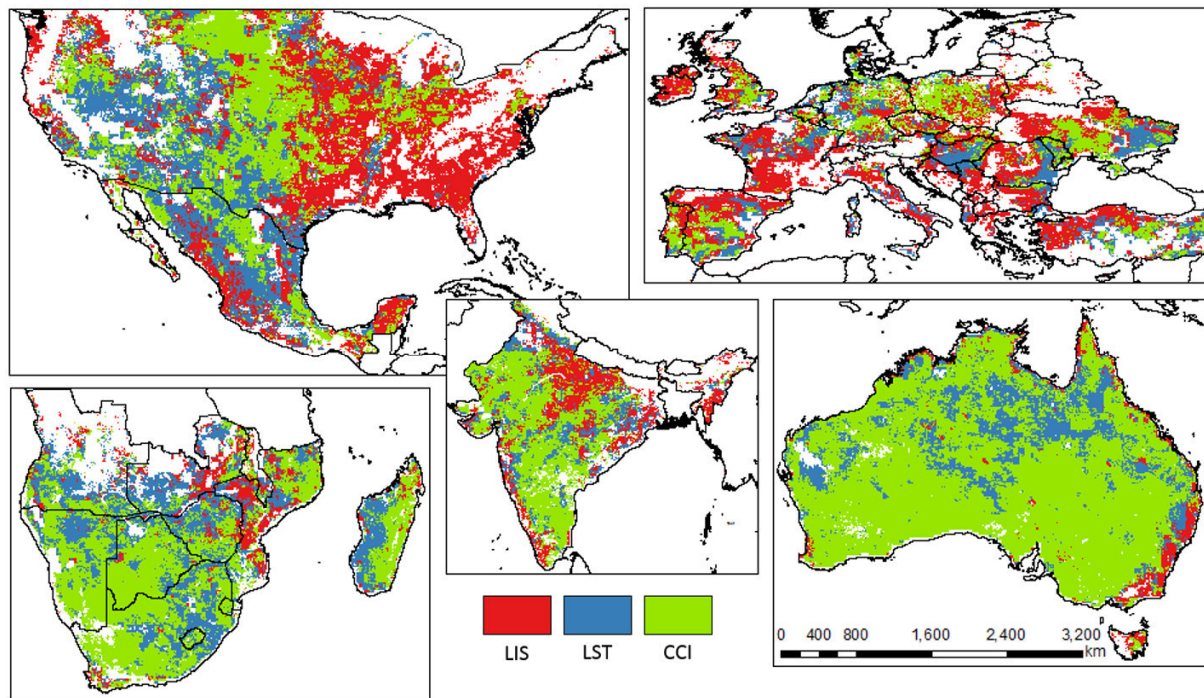


650
651 **Fig. 6.** Spatial distribution of the error variance for the land surface temperature (LST) dataset over the
652 five selected macro-regions.
653



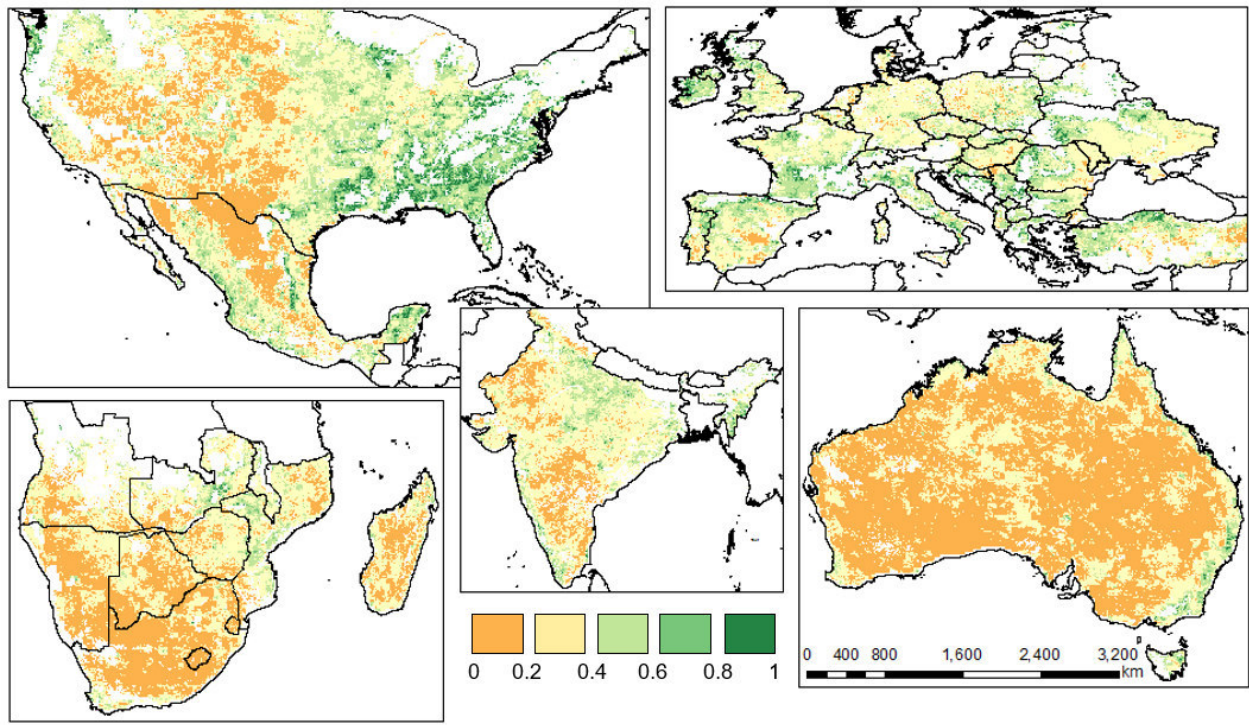
654
 655 **Fig. 7.** Spatial distribution of the error variance for the ESA Climate Change Initiative (CCI) dataset
 656 over the five selected macro-regions.

657



658
 659 **Fig. 8.** Maps representing the best performing (lowest error variance) dataset for each cell according to
 660 the TC analysis.

661

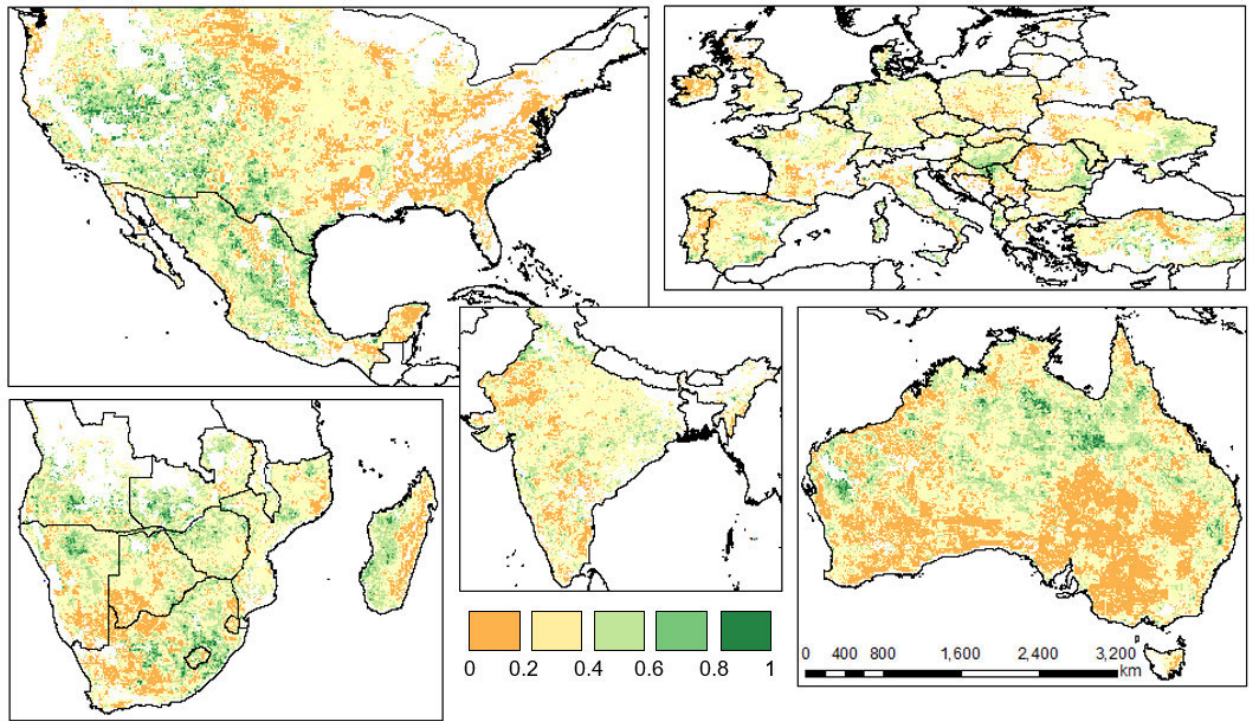


662

663 Fig. 9. Maps representing the ensemble mean weighting factor for the LIS dataset according to the error

664 maps derived from the TC analysis.

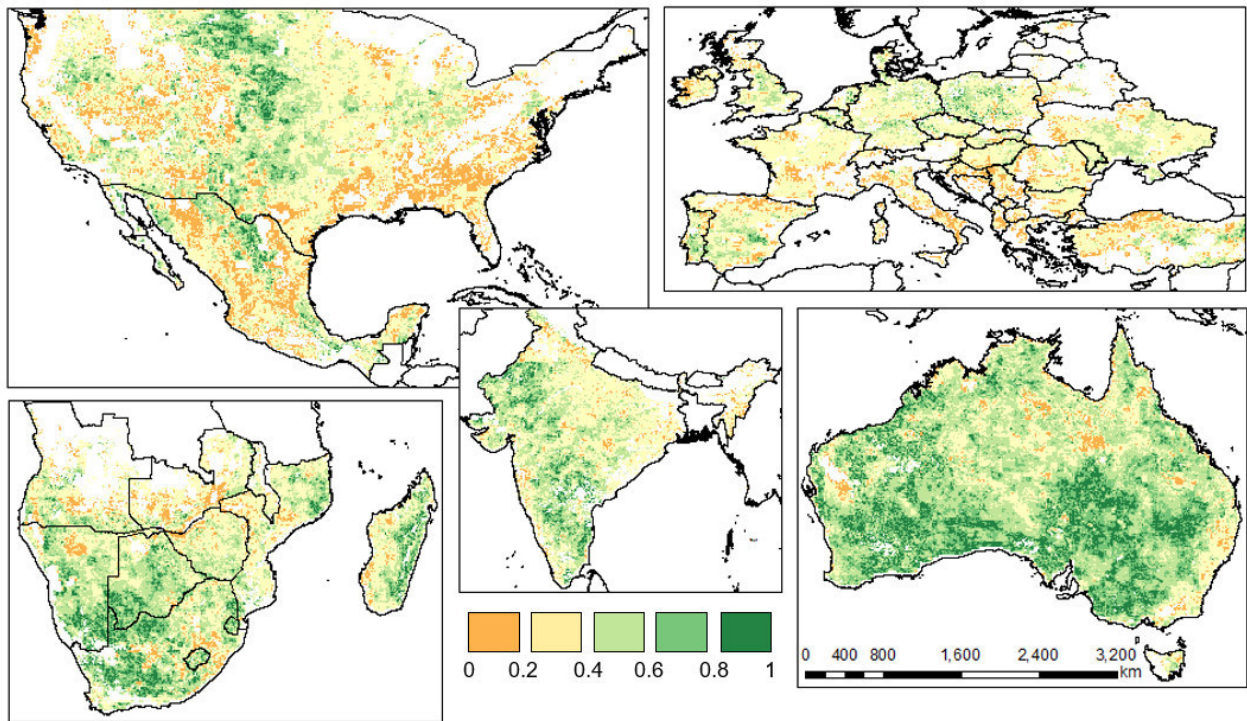
665



666

667 **Fig. 10.** Maps representing the ensemble mean weighting factor for the LST dataset according to the
668 error maps derived from the TC analysis.

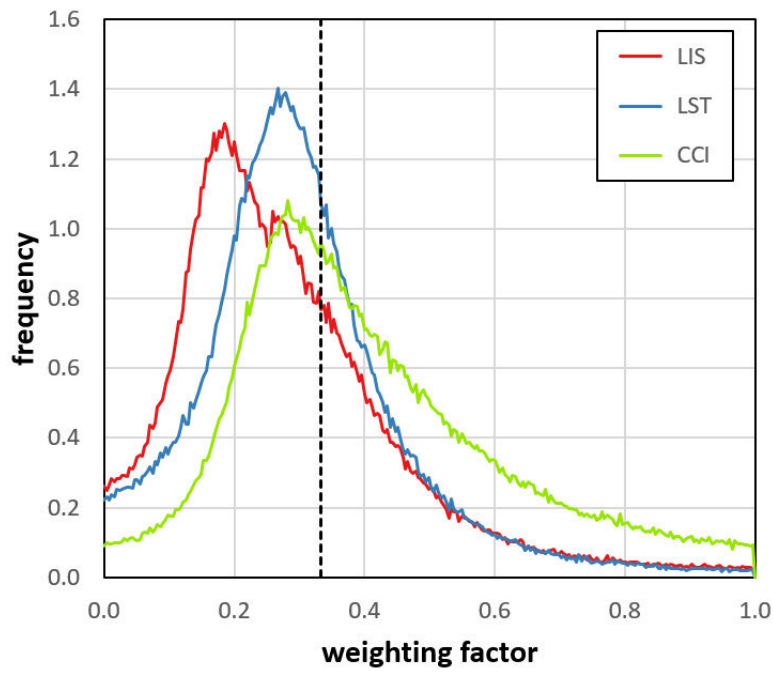
669



670

671 Fig. 11. Maps representing the ensemble mean weighting factor for the CCI dataset according to the
672 error maps derived from the TC analysis.

673



674

675 Fig. 12. Frequency distribution of the ensemble mean weighting factor for each dataset computed
676 according to the TC analysis. The black dotted line represents the value corresponding to a simple
677 arithmetic average (1/3).

678